Structural Study of the DNA Dipalmitoylphosphatidylcholine Complex at the Air−Water Interface

Luigi Cristofolini,*[,†,‡] Tatiana Berzina,[†,‡] Svetlana Erokhina,[†] Oleg Konovalov,[§] and Victor Erokhin[†,‡,||]

Department of Physics, University of Parma, Viale Usberti 7 A, 43100 Parma, Italy, Centro CRS SOFT, c/o Dipartimento di Fisica, Università La Sapienza, Piazzale Aldo Moro 4, 00185 Roma, Italy, European Synchrotron Radiation Facility, 38043 Grenoble Cedex, France, and Institute of Crystallography, Russian Academy of Sciences, Leninsky pr. 59, Moscow, Russia

Received March 21, 2007; Revised Manuscript Received April 19, 2007

We present here results that demonstrate the formation of a complex of DNA with zwitterionic dipalmitoylphosphatidylcholine (DPPC) monolayer at the air−water interface in the presence of Ca^{2+} ions; in particular, we show that the presence of Ca^{2+} cations is essential for the formation of the complex of DPPC with DNA. We characterize the resulting structure by X-ray reflectivity and by null-ellipsometry. We show that DNA maintains its native double helix form when attached to the zwitterionic lipid monolayer, at difference with the case of ammine containing monolayers. Our findings are discussed in view of other works that recently appeared on the interaction of DNA with zwitterionic phospholipids, emphasizing the role of DPPC as a potential vector for transfer of genetic material into mammalian cells by nonviral gene therapy and also suggesting Langmuir/Blodgett layers of zwitterionic phospoholipids as a method for nonconventional DNA immobilization.

Introduction

Investigation of the interaction of DNA with systems similar to biological membranes is important both from fundamental and applied points of view, as it can clarify the role of its interactions with membranes. On the other hand, it can provide a new method of DNA immobilization, for example, for sequencing purposes[1] or for transfer of genetic material into mammalian cells by nonviral gene therapy.[2] In this frame, application of the Langmuir−Blodgett (LB) technique is very suitable because it allows studying systems that can be considered as model membranes. Even more promising seems the study of the Langmuir monolayers at the air/water interface because the situation in this case, given the fluidity of the monolayer, is more similar to the natural conditions. However, special equipment and techniques are necessary as it is much more difficult to study liquid surfaces than solid ones. Synchrotron radiation facilities are among the most powerful tools for such purposes.[3,4]

Most of the structural studies on DNA-containing mono- and multilayers, at the air/water interface as well as transferred onto solid supports, have been performed using cationic amphiphilic molecules.[5] In some cases, in particular, when the amphiphile headgroup contains amine, DNA splitting into single-strand form occurs, while in many other cases DNA remains in its native double-strand form.[6] However, it seems that the interaction of DNA with monolayers of molecules having positively charged headgroups involves mainly electrostatic interactions.[1] It is therefore controversial whether one should expect interaction of DNA with monolayers of zwitterionic molecules, which have only dipolar moment and no net electric charge.

In the present work, we focus on the interaction of DNA with monolayers of zwitterionic natural lipid dipalmitoylphosphatidylcholine (DPPC). We choose DPPC as a prototype because monolayers of this molecule are rather well studied at the air/water interface using also reflectivity measurements with synchrotron radiation facilities[7] and because of its potential as a gene vector in nonviral gene therapy[2] being a nontoxic phospholipid.

Interaction of DNA with lipid monolayers of mixed composition (including DPPC) deposited on solid support has been studied, and the structure of the resulting complex has been characterized in ref 8. However, those authors have concluded that there is practically no interaction with the monolayer when it consists only of DPPC: the reflectivity curves of the layer with and without DNA were practically the same in that case. DNA started to attach to the layer only when cholesterol was added, and the amount of attached DNA was proportional to the amount of cholesterol present in the monolayer. This conclusion seems to be in contrast with some studies of the interaction of DNA with multilamellar liposomes, where DNA is reported to attach to the DPPC headgroups in the presence of Ca^{2+} ions.[9] Thus, one can suppose that the reported absence of DNA interaction with DPPC monolayer was due to the composition of the water subphase.

The aim of the present study is the investigation of the DNA complexation with DPPC monolayer at the air/water interface. Formation of the monolayer and its morphology was investigated by compression isotherm measurements and with Brewster angle microscopy, while the thickness and structure of the complex layer were studied by ellipsometry and X-ray reflectivity measurements.

Experimental Section

DPPC and herring sperm DNA ("crude oligonucleotides", <50 bp, degraded) were purchased from Sigma and were used as supplied.

* To whom correspondence should be addressed. Tel: +39 0521 905276; fax: +39 0521 905223; e-mail: cristofolini@fis.unipr.it.
† University of Parma.
‡ Centro CRS SOFT.
§ European Synchrotron Radiation Facility.
|| Institute of Crystallography Russian Academy of Sciences.

10.1021/bm070322w CCC: $37.00
Published on Web 06/01/2007

A preliminary study of the complex monolayer formation at the air/water interface was carried out on KSV 5000 Langmuir trough. Milli-Q purified water (resistivity more than 18.2 MΩ × cm) was used for the subphase preparation. All monolayers were formed on a subphase with pH 6.0, containing 5 mM $CaCl_2$ and 10 mM NaCl. Compression of the monolayers was performed at a speed of 10 mm/min.

For the ellipsometric measurements, we used a small homemade trough (84 × 305 mm^2 surface), placed directly in the laser (He−Ne λ = 632.8 nm) light path and positioned through micrometric controls. The ellipsometer (OPTREL Multiskop) was aligned to operate in the vertical plane, at an incidence angle $\Phi = 48°$ from the normal to the water surface. The same computer was used to drive the electronics controlling the Langmuir trough and to perform the ellipsometric measurement. Brewster angle microscopy imaging measurements have been performed using the same instrument, at an incidence angle $\Phi = 53°$, while the light was collected with an M-PLAN APO 10× (Mitutoyo) objective and a CCD camera detector, and images were captured with a frame-grabber.

In all the experiments, the water surface was routinely characterized prior to film dispersion by a complete compression cycle. In ellipsometry, one measures the angles Δ and Ψ (defined in the usual way[10] from the reflectivity coefficients R_p and R_s for p- and s-polarized waves: $R_p/R_s = e^{i\Delta} \tan \Psi$. We always measured first the pure water surface (i.e., before film dispersion) to provide the final alignment and quantification of capillary waves, thus providing an accurate reference point. We employed the Drude approximation[10] when a monocomponent film was present. In this approximation, valid for homogeneous and thin films, the angle Ψ is not affected by the film, and its constant value can be used as a check of the overall alignment, while the variation $\delta\Delta$ of the phase-angle Δ is linearly proportional to the film thickness. However, when complex structures are formed, a standard inversion scheme based on Fresnel formulas was applied for the conversion of the measured angles Δ and Ψ into film thickness.

X-ray reflectivity (XRR) curves were measured at the European Synchrotron Radiation Facility (ESRF, Grenoble) using the ID10B (Troika II) beamline. Incident wavelength was $\lambda = 1.489$ Å. To prevent the detector from saturation, at small incidence angle, we used attenuators on the incoming beam (aluminum foils with different thickness, ranging from 0 to 1.1 mm with step of 0.1 mm). The true reflectivity signal was separated from X-ray diffuse scattering by taking rocking curves or off-specular scans. Scans were terminated when the specular reflection and diffuse scattering in its vicinity became equal. A Langmuir trough with a single moving barrier (maximum surface 418 × 170 mm^2) was mounted on an active antivibration support (Halcyonics, Germany) and was surrounded by helium atmosphere to reduce diffuse scattering from air. To check the alignment and to provide a reference, the XRR from the bare water surface was measured before all measurements on Langmuir films.

For the XRR measurements, two series of experiments were performed. First, measurements were acquired on DPPC monolayers, spread and compressed on the subphase without DNA as described above. In the second case, the monolayers were formed on the subphase which contained also DNA at a final concentration of 5 μg/mL. First, acquisition and further compression were performed after an equilibration time of 40 min. In each series, XRR measurements were carried out on monolayers compressed up to 10, 20, and 30 mN/m.

The reflectivity data were subsequently analyzed with our own software, developed in the Matlab computing environment, which calculates the reflectivity curve for a given model according to the so-called "Parratt recursive approach".[3,11] In this case, one calculates the transmission and reflection Fresnel coefficients at each interface. To reproduce the reflectivity curve of a real multilayer, a structured model of independent layers, each with uniform electron density, has to be provided. Roughness of real layers is accounted for using the Névot−Croce approximation,[12] which implies scaling of the reflectivity at the interface between layers *a* and *b* by a pseudo Debye−Waller factor $\exp(-2k_a k_b \sigma^2)$, σ being the roughness root mean square (rms) value, and $k_a k_b$ representing the *z*-component of the wave vector for layers a and b, respectively. The quality of the fit is evaluated weighting the discrepancy between data and model either by the uncertainty of the data (true χ^2 test) or by a factor which is inversely proportional to the reflectivity itself. The latter strategy gives comparatively more weight to the high-*Q* data, which, albeit affected by larger uncertainty, contain more physical information.

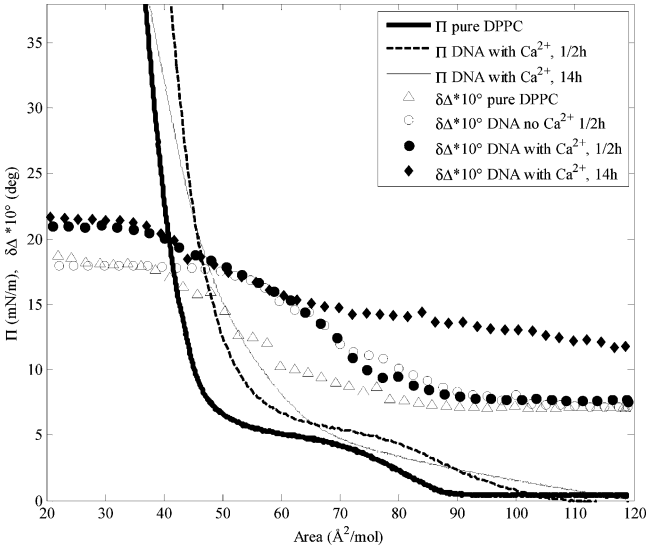

Figure 1. Combined pressure−area and pressure−thickness "ellipsometric" isotherms for DPPC alone, DPPC in the presence of DNA with no Ca^{2+} ions, and DPPC in the presence of DNA and Ca^{2+} ions for different incubation times: $^1/_2$ h and 14 h. Continuous thick line: surface pressure versus area per molecule, for DPPC alone. Dashed thick line: surface pressure versus area per molecule, for DPPC on DNA subphase, after $^1/_2$ h of incubation. Continuous thin line: same after 14 h of incubation. Empty triangles: variation of the ellipsometric phase angle $\delta\Delta$ for DPPC alone. Empty circles: $\delta\Delta$ for DPPC on DNA without Ca^{2+} ions. Filled circles: $\delta\Delta$ for DPPC on DNA with Ca^{2+} ions after $^1/_2$ h incubation time. Filled diamonds: same after 14 h of incubation.

Results and Discussion

Compression Isotherms, Ellipsometry, and Imaging. Surface pressure−area isotherms are shown as continuous lines in Figure 1 for DPPC with NaCl and $CaCl_2$ but no DNA and for DPPC on DNA containing subphase with time intervals of $^1/_2$ h and 14 h before compression, respectively. As known from the literature,[13] DPPC exhibits a plateau, which corresponds to the transition from a liquidlike to a compressed phase. In the presence of DNA, and for incubation time of $^1/_2$ h, the curve is shifted by 5 $Å^2$ toward larger area per molecule, and moreover, the plateau is smeared. In the case of long incubation time (14 h), one observes the complete disappearance of the plateau and a slower increase of the isotherm in the compressed region, implying a softer monolayer (the compression modulus being $\epsilon = -A\partial\Pi/\partial A$). This suggests that the attachment of DNA to DPPC increases the effective molecular area, and during the compression, the molecules start to interact with each other via the attached DNA strands at much longer distance than they would without DNA. The interaction occurring in the expanded region of the isotherm is in part similar to that of lipid monolayers in nonspecifical interaction with neutral polymers,[14] however, the behavior in the compressed region is different, as the isotherm in the presence of DNA is shifted toward larger area per molecule. We can also make a comparison with the interaction of myelin basic protein (MBP), a positively charged,

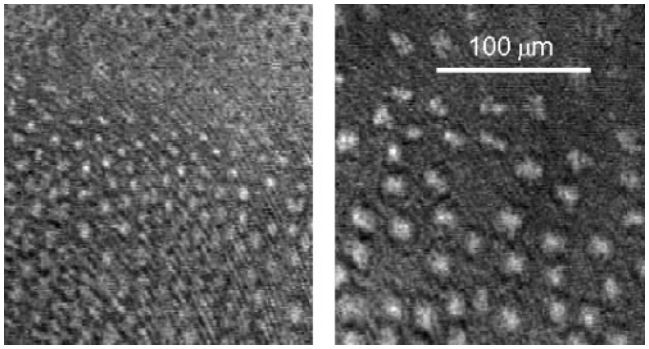

Figure 2. BAM images taken at an area of 71 Å^2 per molecule, i.e., in the plateau in the compression isotherms (see Figure 1) for DPPC alone (left panel) and DNA−DPPC complex (right panel). The size domain increased in the presence of DNA. A scale bar of 100 μm is provided for reference.

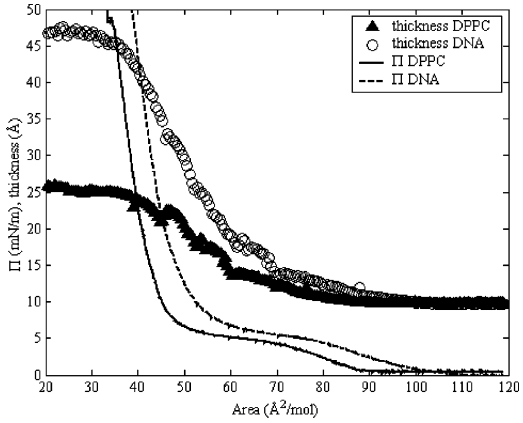

Figure 3. Thickness of the monolayer as a function of the area per molecule, as deduced from the ellipsometric measurement (see text), for DPPC (filled triangles) and for the DNA−DPPC complex layer (empty circles). The surface pressure−area isotherm is also shown for comparison for DPPC (thick line) and DNA−DPPC complex (dashed line).

intrinsically unstructured protein, with different phospholipid monolayers. In the presence of negatively charged DPPS and DPPG, the electrostatic interaction appears to be the driving force, with intimate association of MBP with the headgroups and formation of protein−lipid complexes. On the contrary, in the presence of zwitterionic DPPC, already at low pressure the protein seems to penetrate among the lipid domains,[15] which retain their character. The DNA situation seems to be more similar to the DPPC case than to the anionic lipid layers, suggesting some kind of generality to the observed process.

Prior to performing null-ellipsometry measurements, we controlled the film homogeneity and characterized the eventual domain morphology by Brewster angle microscopy (BAM). Typical pictures taken during the plateau in the compression isotherms (namely, at an area of 71 Å^2 per molecule) are shown for DPPC alone and DNA−DPPC complexes in Figure 2, left and right panels, respectively. In agreement with the literature,[16] domains were observed only in the plateau region of the isotherm, and the domain size increased in the presence of DNA, as shown in Figure 2. This effect is opposite to that encountered in DMPE exposed to DNA and divalent cations, which makes the domains "smaller, fuzzy, more frayed and dendrite-like".[17] However, our findings could be explained by taking into account the contrast between the tendency of the lipid chains of DPPC to form aggregates at the expense of the electrostatic cost of packing the dipolar heads: when DPPC alone is present, small domains are obtained, but the addiction of the negatively charged DNA bound via the Ca^{2+} cations reduces the electrostatic cost of packing the polar heads, thus favoring the formation of larger domains.

Film thickness was probed by the variation of the ellipsometric phase-angle $\delta\Delta$ which, in the Drude approximation,[10] is linearly proportional to film thickness. In Figure 1, with plot symbols, we report the variation $\delta\Delta$ against the area per molecule: for DPPC with NaCl but in the absence of DNA or in the presence of DNA and NaCl but in the absence of Ca^{2+} cations (open triangles and open circles, respectively), the DPPC film formation can be followed along the compression isotherm. When DNA, NaCl, and Ca^{2+} cations are simultaneously present in the subphase (filled circles and filled diamonds), the film thickness increases with respect to the case of DPPC alone, presumably because of the attachment of DNA molecules under the DPPC layer. This effect of DNA "attachment" is present only if the Ca^{2+} cations are present. If only the NaCl is present, but no Ca^{2+} is present, DNA does not form the complex with the Langmuir layer of DPPC.

We can quantify the thickness of the DPPC layer and of the DNA−DPPC complex from the ellipsometric angle Δ in the Drude approximation: in Figure 3, the filled triangles represent the pure DPPC film thickness, extracted from $\delta\Delta$. In principle, in the condensed phase of DPPC, one should consider the uniaxial anisotropy of the refractive index. However, such anisotropy is extremely small, amounting roughly to 3%; moreover, as mentioned in the Experimental Section, we work at a single angle of incidence, and therefore for our purposes, it suffices to consider the isotropic mean value[18] of the refractive index $n = ({}^2/_3 n_x + {}^1/_3 n_z) = 1.453$. A further, and more important, approximation consists in ignoring the dependence of the refractive index from molecular packing along the compression isotherm. The resulting thickness, as shown in Figure 3, reaches the plateau value of 25 Å in the compressed phase, in nice agreement with the value determined by X-ray reflectivity (see below).

Inspection of Figure 1 clearly shows that the presence of DNA increases the variation of the angle Δ; however, to determine precisely the DNA layer thickness, one should know exactly what is its refractive index, which in turn depends on the fractional coverage of the lipid monolayer by DNA. As a first rough approximation, we proceed as follows: from the X-ray reflectivity data (see below), we obtain a volume density of DNA in water at most 30%, therefore, we assume for the refractive index value a linear combination of the values of pure water ($n = 1.33$) and of pure double-stranded DNA[19] ($n = 1.55$), that is, $n = 1.40$. With this assumption, we would estimate the DNA layer thickness to only 12 Å, a value much smaller than that determined more precisely by X-ray reflectivity. However, such a result depends strongly on the DNA content: for example, a reduction of DNA content to 20% would imply a value for the refractive index $n = 1.37$, and 20 Å of thickness for the DNA sublayer, which is perfectly compatible with the X-ray reflectivity datum. In Figure 3, we report therefore the DNA sublayer film thickness calculated in the latter approximation.

X-ray Reflectivity. Reflectivity curves of DPPC on subphases either containing or not containing DNA have been registered at $\Pi = 10$, 20, and 30 mN/m and are shown as filled circles and empty triangles, respectively, in the three panels of Figure 4, normalized to the Fresnel reflectivity of pure air/water interface. Some consequences of DNA intercalation are evident

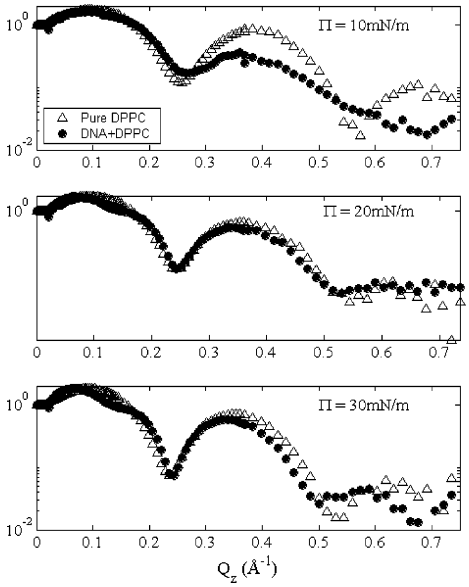

Figure 4. Reflectivity curves of DPPC on subphases both containing (filled circles) and not containing DNA (empty triangles) measured at $\Pi = 10$, 20, and 30 mN/m (top, middle, and bottom panel, respectively) normalized to the Fresnel reflectivity of pure air/water interface. Note, at 10 mN/m the shift of the position of the first minimum, from $Q_z = 0.25$ Å^{-1} to 0.27 Å^{-1} and at the higher pressures the onset of a depression around $Q_z = 0.12$ Å^{-1}.

even prior to modeling the data: at the lowest pressure, the presence of DNA in subphase produces a moderate shift of the position of the first minimum, from $Q_z = 0.25$ Å^{-1} to 0.27 Å^{-1}, and a pronounced smearing of the overall curve, indicating small reduction of film thickness, together with some loss of contrast. On the contrary, at the higher pressures, the position of the first minimum is unaffected, but a depression is induced around $Q_z = 0.12$ Å^{-1}, indicating that some film structuration is developing on a scale larger than the original phospholipid film thickness.

The reflectivity profiles of phospholipid alone have been fitted by a two-slab model, representing the phosphatidic head and the lipid tail, respectively. The results are reported in the first part of Table 1. The thickness of both polar head and alkyl tail regions is constant within the accuracy of the determination, corresponding to a total film thickness of 23−24 Å, a value somewhat reduced with respect to that reported[20] for DPPC on ultrapure water, 25.3(4) Å, but in perfect agreement with other studies on a similar, salt-containing, subphase (see, e.g., refs 8 and 16) confirming the general effect of salt content in determining the molecular packing. Also, the electron density slightly increases with the pressure, in agreement with the fact that the measurements were done at and above the plateau in the isotherm, where the film consists of domains of closely packed molecules, whose density increases with the pressure (as confirmed independently also by our BAM imaging).

The parameters determined on DPPC have been used as a starting point in the subsequent fit of the reflectivity curves measured in the presence of DNA, which are well reproduced by a three-slab model: alkyl chains, phosphatidic heads, and DNA. In the panels A, B, and C of Figure 5, we show the corresponding fits of reflectivity profiles, measured at $\Pi = 10$, 20, and 30 mN/m, respectively, with the parameters reported in the second part of Table 1. We note in passing the very high quality of the fitting, which invariably results in a χ^2 always smaller than 2 and sometimes smaller than 1. The corresponding models are shown in the insets of the same figures. The maximum in the electron density profile found at the depth of

Table 1. Parameters Obtained by the Least-Square Fit of the Reflectivity Profiles by the Parratt Algorithm[a]

Pure DPPC				
		tails	heads	subphase
		$\Pi = 10$ mN/m		
el. density ρ	(el/Å^3)	0.344	0.530	0.334
thickness	(Å)	17.4	4.7	infinite
roughness σ	(Å)	3.0	4.1	2.8
		$\Pi = 20$ mN/m		
el. density ρ	(el/Å^3)	0.338	0.546	0.334
thickness	(Å)	17.8	5.7	infinite
roughness σ	(Å)	3.1	5.4	3.7
		$\Pi = 30$ mN/m		
el. density ρ	(el/Å^3)	0.344	0.551	0.334
thickness	(Å)	18.2	5.3	infinite
roughness σ	(Å)	3.4	4.3	3.6

DPPC on DNA Subphase					
		tails	heads	DNA	subphase
		$\Pi = 10$ mN/m			
el. density ρ	(el/Å^3)	0.336	0.499	0.380	0.334
thickness	(Å)	15.5	3.6	6.3	infinite
roughness σ	(Å)	3.1	4.3	2.8	2.2
		$\Pi = 20$ mN/m			
el. density ρ	(el/Å^3)	0.343	0.552	0.373	0.334
thickness	(Å)	18.0	6.0	26.7	infinite
roughness σ	(Å)	3.2	6.7	3.8	5.0
		$\Pi = 30$ mN/m			
el. density ρ	(el/Å^3)	0.342	0.616	0.385	0.334
thickness	(Å)	21.6	4.6	25.1	infinite
roughness σ	(Å)	3.3	5.6	4.2	5.7

[a] For the phospholipid alone, top part of the table, we used a two-slab model, representing the phosphatidic head and the lipid tail, as described in the text. For the phospholipid on DNA subphase, bottom part of the table, a third layer, representing DNA, was added. We studied the films at three different surface pressures; the relevant parameters (slab thickness, electron density, and surface roughness) are reported separately for each value of surface pressure. The abbreviation el. represents electron.

20 Å corresponds to the electron-rich lipid heads. In panel D of Figure 5, we show an artist's impression of the model obtained by fitting the X-ray reflectivity data for DPPC−DNA interaction.

At the highest pressures, the overall thickness of DPPC film is basically unaffected by the presence of DNA, which is concentrated in a layer attached below the DPPC film, with thickness 25−26 Å. Such a value implies that DNA is in the double-stranded form (for the correlation between film thickness and multiplicity of the helix see, e.g., ref 21) at difference from the case of amine containing amphiphiles, such as octadecylamine (ODA), where DNA splitting was found,[6] but also of mixed DPPC and synthetic charged DC-cholesterol in the absence of Ca^{2+} ions[8] which exhibit a smaller thickness, implying single-stranded form for DNA, and in analogy with the results obtained on hexadecyltrimethylammonium bromide (HTAB) monolayers.[6]

The electron density found for the DNA region $\rho = 0.380$-(5) el/Å^3 is in agreement with that reported in the literature for DNA under a DMPE layer,[17] but we have reason to believe that it does not correspond to a pure DNA layer. In the presence of ODA, we have observed a layer of a much higher electron density, namely, $\rho = 0.496(5)$ el/Å^3 at the same surface pressure. Assuming that the latter value would correspond to pure DNA

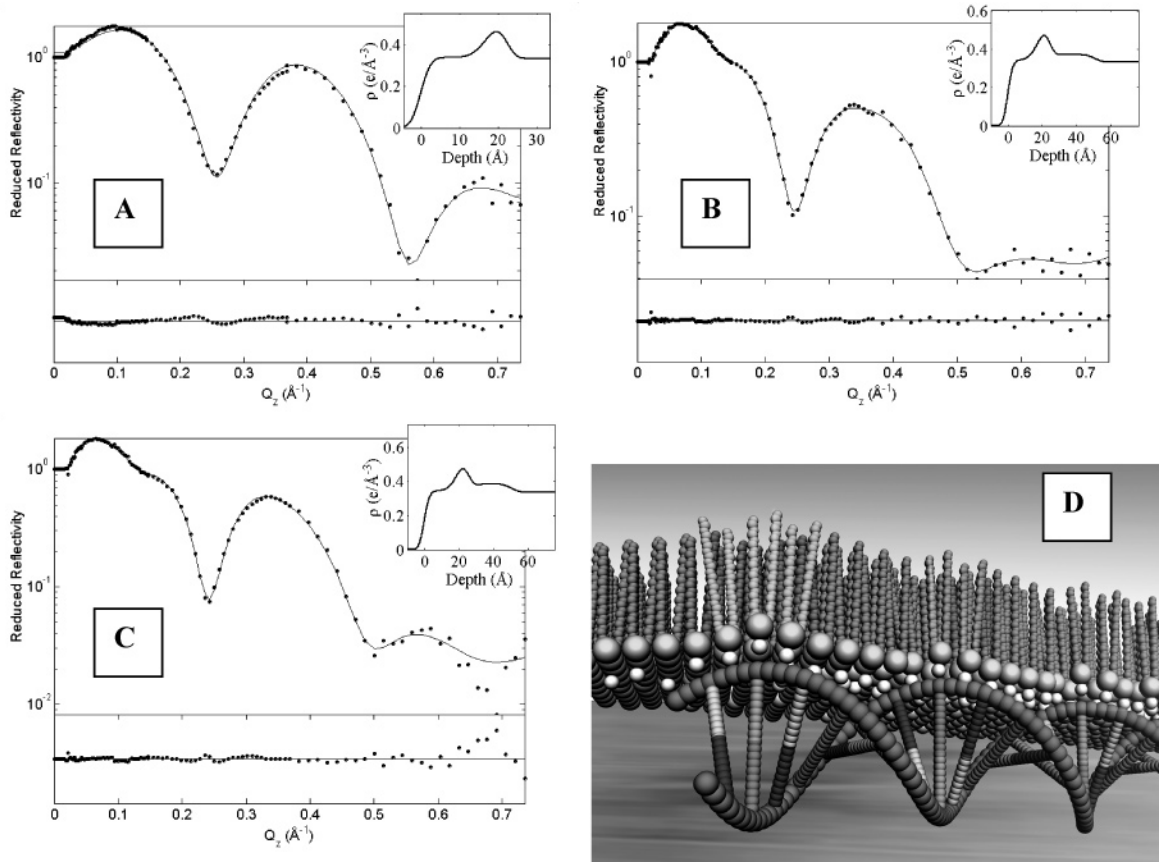

Figure 5. (A) Top panel: points represent the measured reflectivity of DPPC on DNA containing subphase at $\Pi = 10$ normalized to the Fresnel reflectivity of pure air/water interface. The continuous line in the same panel is the reflectivity calculated with the best fit model (see text). The bottom panel contains the deviations. Note the excellent quality of the fit. The inset in the upper corner represents the electron density profile (in electrons per Å^3) of the model used to fit the experimental curve. The maximum in the electron density profile found at the depth of 20 Å corresponds to the electron-rich lipid heads. (B) Measured and calculated reflectivity, deviations, and fitting model for the same as above, at the surface pressure $\Pi = 20$ mN/m. (C) Measured and calculated reflectivity, deviations, and fitting model for the same as above, at the surface pressure $\Pi = 30$ mN/m. (D) An artist's impression of the model obtained by fitting the X-ray reflectivity data for DPPC−DNA interaction.

(which is questionable), we calculate that the layer composition is about 30% DNA and 70% water, corresponding to a situation of partial coverage. The real DNA content could even be smaller, as we have no independent indication that the coverage under the ODA layer was 100% DNA. Neutron reflectivity measurements could help to clarify this point.

Interestingly, at the pressure of 10 mN/m, the framework is rather different: DNA seems to induce a reduction of the phospholipid film thickness from 22 to 20 Å. To understand this point, one must take into account the fact that at such pressure we have a plateau in the isotherm; the presence of DNA simply induces dense packing of the film, which is probably of mixed composition. Therefore, the area per molecule is larger than that at the same pressure for DPPC alone, possibly resulting in a more pronounced molecular tilting.

Conclusions

Our results demonstrate the formation of a complex of DNA with zwitterionic DPPC monolayer at the air−water interface in the presence of Ca^{2+} ions. We have also shown that the presence of Ca^{2+} is essential for the formation of the complex. We characterized the structure of the resulting complex, showing that DNA maintained its native double helix form when attached to the DPPC monolayer and that DNA covers about 20−30% of the surface area.

Therefore, the absence of DPPC−DNA interaction reported in the only work on DNA containing DPPC LB films can be attributed to the particular subphase employed, not containing divalent ions, which are known to be necessary for the complex formation.[22]

Most of our results are consistent with those very recently reported for monolayers made by another zwitterionic lipid, namely, DMPE,[17] and are in line with the observations on the different mechanisms of interaction between lipid monolayers and neutral polymers.[14] A similarity is also found with the case of the interaction of MBP, a charged intrinsically unstructured protein with zwitterionic phospholipid layers,[15] suggesting some kind of generality of the interaction mechanism observed.

Our findings suggest that zwitterionic phospholipids such as DPPC could be useful as potential vectors for transfer of genetic material into mammalian cells by nonviral gene therapy. Moreover, the possibility of determining the attachment of DNA to Langmuir layers of zwitterionic phospoholipids by controlling the presence of divalent cations in the subphase suggests a new method for nonconventional DNA immobilization, for example, for sequencing purposes.

Acknowledgment. We acknowledge the European Synchrotron Radiation Facility for provision of beam time. The authors are grateful to Mr. Yuri Gunaza for the help in the preparation of some figures, to Dr. Claudia Folli and

Dr. Silvia Folloni (Dipartimento di Biochimica e Biologia Molecolare, Universitá di Parma) for help in the characterization of the DNA samples used for the experiments, and to Prof Marco Fontana for many useful and stimulating discussions.

References and Notes

(1) Wang, J.; Bard, A. J. *Anal. Chem*. **2001**, *73*, 2207−2212. Dufva, D. *Biomol. Eng.* **2005**, *22*, 173−184. Pannier, A. K.; Brian, C.; Anderson, B. C.; Shea, D. *Acta Biomater.* **2005**, *1*, 511−522. Cantor, C. R.; Schimmel, P. R. *Biophysical Chemistry;* Freeman: San Francisco, CA, 1980.
(2) Mahato, R. I.; Smith, L. C.; Rolland, A. *Adv. Genet.* **1999**, *41*, 95.
(3) Daillant, J.; Gibaud, A. *X-Ray and Neutron Reflectivity: Principles and Applications;* Springer: Berlin, 1999.
(4) Gibaud, A.; Hazra, S. *Curr. Sci*. **2000**, *78*, 1467−1477. Majewski, J.; Kuhl, T. L.; Kjaer, K.; Gerstenberg, M. C.; Als-Nielsen, J.; Israelachvili, J. N.; Smith, G. S. *J. Am. Chem. Soc*. **1998**, *120*, 1469−1473. Fradin, C.; Luzet, D.; Braslau, A.; Alba, M.; Muller, F.; Daillant, J.; Petit, J. M.; Rieutord, F. *Langmuir* **1998**, *14*, 7327−7330. Vaknin, D. J. *Am. Chem. Soc*. **2003**, *125*, 1313−1318.
(5) . Erokhin, V.; Popov, B.; Samori, B.; Yakovlev, A. *Mol. Cryst. Liq. Cryst*. **1992**, *215*, 213−220. Sukhorukov, G.; Erokhin, V.; Tronin, A. *Biofizika* **1993**, *38*, 257−262. Okahata, Y.; Tanaka, K. *Thin Solid Films* **1996**, *284−285*, 6−8. Shabarchina, L. I.; Montrel, M. M.; Sukhorukov, G. B.; Sukhorukov, B. I. *Thin Solid Films* **2003**, *440*, 217−222. Kago, K.; Matsuoka, H.; Yoshitome, R.; Yamaoka, H.; Ijiro, K.; Shimomura, M. *Langmuir* **1999**, *15*, 5193−5196. Symietz, C.; Schneider, M.; Brezesinski, G.; Mohwald, H. *Macromolecules* **2004**, *37*, 3865−3873.
(6) . Erokhina, S.; Berzina, T.; Cristofolini, L.; Konovalov, O.; Erokhin, V.; Fontana, M. P. *Langmuir* **2007**, *23*, 4414−4420.
(7) . Brezesinski, G.; Thoma, M.; Struth, B.; Mohwald, H. *J. Phys. Chem.* **1996**, *100*, 3126−3130. Haas, H.; Caetano, W.; Borissevitch, G. P.; Tabak, M.; Mosquera Sanchez, M. I.; Oliveira, O. N.; Scalas, E.; Goldmann, M. *Chem. Phys. Lett.* **2001**, *335*, 510−516. Estrela-Lopis, I.; Brezesinski, G.; Möhwald, H. *Chem. Phys. Lipids* **2004**, *131*, 71−80.
(8) . Wu, J. C.; Lin, T. L.; Jeng, U. S.; Lee, H. Y.; Gutberlet, T. *Physica B* **2006**, *385−386*, 841−844.
(9) McManus, J. J.; Radler, J. O.; Dawson, K. A. *Langmuir* **2003**, *19*, 9630−9637.
(10) Tompkins, H. G. *A User's Guide to Eellipsometry;* Academic press: Boston, MA, 1993.
(11) Parratt, L. G. *Phys. Rev.* **1954**, *95*, 359−369.
(12) Nevot, L.; Croce, P. *Rev. Phys. Appl*. **1980**, *15*, 761−779.
(13) Slotte, J. P.; Mattjus, P. *Biochim. Biophys. Acta* **1995**, *1254*, 22−29.
(14) Ariga, K.; Shin, J. P.; Kunitake, T. *J. Colloid Interface Sci*. **1995**, *170*, 440−448.
(15) Cristofolini, L.; Fontana, M. P.; Serra, F.; Fasano, A.; Riccio, P.; Konovalov, O. *Eur. Biophys. J.* **2005**, *34*, 1041.
(16) Polverini, E.; Arisi, S.; Cavatorta, P.; Berzina, T.; Cristofolini, L.; Fasano, A.; Riccio, P.; Fontana, M. P. *Langmuir* **2003**, *19*, 872.
(17) Wu, J. C.; Lin, T. L.; Yang, C. P.; Jeng, U. S.; Lee, H. Y.; Shih, M. C. *Colloids Surf., A: Phys. Eng. Aspects* **2006**, *284*, 103−108.
(18) Gromelski, S.; Brezesinski, G. *Langmuir* **2006**, *22*, 6293−6301.
(19) Thoma, M.; Schwendler, M.; Baltes, H.; Helm, C. A.; Pfohl, T.; Riegler, H.; Mohwald, H. *Langmuir* **1996**, *12*, 1722−1728
(20) Elhadj, S.; Singh, G.; Saraf, R. F. *Langmuir* **2004**, *20*, 5539−5543.
(21) Vaknin, D.; Kjaer, K.; Alsnielsen, J.; Losche, M. *Biophys. J.* **1991**, *59*, 1325−1332.
(22) Shabarchina, L. I.; Montrel, M. M.; Sukhorukov, G. B.; Sukhorukov, B. I. *Thin Solid Films* **2003**, *440*, 217−222. Sukhorukov, G. B.; Montrel, M. M.; Petrov, A. I.; Shabarchina, L. I.; Sukhorukov, B. I. *Biosens. Bioelectron.* **1996**, *11*, 913−922.
(23) Budker, V. G.; Godovikov, A. A.; Naumova, L. P.; Slepneva, I. A. *Nucleic Acids Res.* **1980**, *8*, 2499. Bailey, A. L.; Sullivan, S. M. *Biochim. Biophys. Acta* **2000**, *1468*, 239. McLoughlin, D.; Dias, R.; Lindman, B.; Cardenas, M.; Nylander, T.; Dawson, K.; Miguel, M.; Langevin, D. *Langmuir* **2005**, *21*, 1900.

BM070322W